

the selectivity filter and would regulate open probability at the pore by modulating K⁺ occupancy.

Brickley SG, Aller MI, Sandu C, Veale EL, Alder FG, Sami H, Mathie A, & Wisden W (2007). *J Neurosci* 27, 9329-9340.

Kim Y, Bang H, & Kim D (2000). *J Biol Chem* 275, 9340-9347.

Niemeyer MI, González-Nilo FD, Zúñiga L, González W, Cid LP, & Sepúlveda FV (2007). *Proc Natl Acad Sci U S A* 104, 666-671.

Rajan S, Wischmeyer E, Liu GX, Preisig-Muller R, Daut J, Karschin A, & Derst C (2000). *J Biol Chem* 275, 16650-16657.

Warth R, Barrière H, Meneton P, Bloch M, Thomas J, Tauc M, Heitzmann D, Romeo E, Verrey F, Mengual R, Guy N, Bendahhou S, Lesage F, Poujeol P, & Barhanin J (2004). *Proc Natl Acad Sci U S A* 101, 8215-8220.

Where applicable, the authors confirm that the experiments described here conform with The Physiological Society ethical requirements.

C3

Sodium-dependent regulation of ENaC by apical P2 receptors in rat collecting duct: are P2X receptors luminal sodium sensors?

S.S. Wildman^{1,2}, D.G. Shirley², B.F. King² and R.J. Unwin²

¹*Veterinary Basic Sciences, Royal Veterinary College, London, UK* and ²*Physiology and Nephrology, UCL, London, UK*

The epithelial Na⁺ channel (ENaC) plays a major role in the regulation of Na⁺ balance and blood pressure by controlling Na⁺ reabsorption along the renal collecting duct (CD). ENaC activity is inhibited by P2 receptors (P2Rs) which are activated by extracellular nucleotides. However, uncertainties exist over the mechanism of inhibition, the P2R subtype(s) involved and molecular pathway(s) activated. This study has addressed the relationship between apical P2Rs and ENaC inhibition in the rat CD.

Kidneys from terminally anaesthetized adult Sprague-Dawley rats, which had been maintained on a low (0.01%) Na⁺ diet (for 10-days in order to increase CD ENaC expression), were microdissected and isolated CD segments were split-open to expose the apical membrane of individual principal cells (PCs). PCs (*in situ*) were studied under voltage-clamp conditions ($V_h = -60$ mV) using the whole-cell perforated-patch clamp technique.

Apically-applied ATP, ATP γ S, UTP and 2meSATP each evoked inward currents (≤ 500 pA; 10 μ M; $n = 10$), whereas 2meSADP and BzATP were inactive (10 μ M; $n = 10$). Currents evoked by 2meSATP were insensitive to DIDS (100 μ M; $n = 5$) and shown to be cationic, consistent with P2X channel activation. Currents evoked by UTP were abolished by DIDS ($n = 5$), consistent with P2Y receptor activation of Ca²⁺-dependent Cl⁻ currents.

Within 3 minutes, nucleotide evoked inward currents significantly reduced the amplitude of subsequent ENaC-mediated currents over a wide range of holding voltages (between 30-60%;

$P < 0.05$) without changing the inward rectification or reversal potential ($n = 12$). Lowering extracellular Na⁺ concentration from 145 to 50 mM failed to alter the degree of inhibition caused by UTP-evoked currents, however 2meSATP-evoked responses instead potentiated the amplitude of the ENaC-mediated current-voltage relationships (75%; $n = 7$). 2meSATP-mediated potentiation of ENaC currents was abolished by wortmannin (100 nM; $n = 3$).

When taken together with previously reported immunohistochemical data (Chapman *et al.* 2006), these biophysical and pharmacological data suggest that ENaC activity is inhibited by apical P2Y₂ and/or P2X₄ and/or P2X₄ and/or P2X_{4/6} receptors when extracellular Na⁺ concentrations are high (145 mM; $n = 12$) but apical P2X₄ and/or P2X_{4/6} receptors switch to potentiators of ENaC activity (involving PI3K) when extracellular Na⁺ is lowered (to 50 mM; $n = 5$). We propose that P2X₄ and/or P2X_{4/6} receptors function as apical Na⁺ sensors responsible for local regulation of ENaC activity in the CD and could thereby regulate Na⁺ balance and systemic blood pressure.

Chapman *et al.* (2006) *Proc Physiol Soc* 2, PC7.

Supported by British Heart Foundation and St Peter's Trust.

Where applicable, the authors confirm that the experiments described here conform with The Physiological Society ethical requirements.

C4

Imaging primary cilia on MDCK cells using atomic force microscopy

J. Evangelides¹, D.N. Sheppard² and T.J. McMaster¹

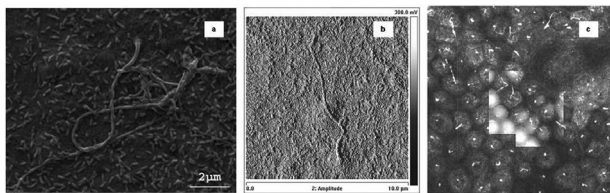
¹*H. H. Wills Physics Laboratory, University of Bristol, Bristol, UK* and ²*Department of Physiology and Pharmacology, University of Bristol, Bristol, UK*

Primary cilia are solitary, immotile, hair-like structures that protrude from the apical membrane of kidney epithelial cells into the cavity of the nephron. The function of the primary cilia was originally unknown, however recent work [1] has identified a link between primary cilia malfunction and autosomal dominant polycystic kidney disease (ADPKD). This malfunction suggests these organelles might act as flow sensors, signalling changes in luminal flow to control transepithelial ion transport along the nephron. Here we have adopted an interdisciplinary approach to investigate the structure and functionality of the primary cilium. We have imaged both Type I and Type II MDCK cells, using scanning electron microscopy (SEM) and atomic force microscopy (AFM). Cells were grown on glass coverslips and fixed with 2% glutaraldehyde in PBS. SEM was used to observe the density of cells and cilia, prior to AFM images being obtained of primary cilia on Type II MDCK cells.

Live cells were imaged under liquid, and as the cilia remain mobile and not adherent to a substrate, their movement and orientation may affect the motion of the AFM cantilever. We found that it was possible to image unfixed cilia using AFM, by removing the cilia from the cell surface. We have achieved this by using

a 'peel-off' method [2] whereby a poly-L-lysine-coated coverslip, placed on top of a layer of cells in a Petri dish, is removed in a single movement, and then imaged *in situ*. The nanoscale surface structure of the immobilised cilia can then be imaged with the AFM. From an analysis of AFM data, we have estimated cilium flexibility, and have probed cilium elasticity using AFM in a nanomechanical mode. By correlating AFM images with single-point AFM force curves, we observe a clear difference in stiffness between the cilium and the cell surface.

Using a combined AFM/confocal microscope we have correlated the structures imaged by AFM, to fluorescent markers for tubulin and actin. The staining observed by confocal microscopy confirms that the structures protruding from the cells in the AFM images are the primary cilia. In a further development, we will report preliminary results from a combination of AFM imaging and patch-clamp electrophysiology to probe how cilium bending is coupled to ion transport.



(a) SEM image (2 μm) of primary cilia on fixed MDCK cells; (b) AFM image (10 μm) of primary cilia on fixed MDCK cells; and (c) Combined confocal (immunofluorescence for tubulin and actin) and AFM images, the latter present as an overlay in the centre of the confocal image.

1. Ong AC and DN Wheatley (2003). The Lancet 361(9359), 774-776.
2. Huang BQ et al. (2006). Am J Physiol Gastrointest Liver Physiol 291, G500-509.

Where applicable, the authors confirm that the experiments described here conform with The Physiological Society ethical requirements.

C5

The cilium-dependent flow-response is amplified by nucleotide release in MDCK cells

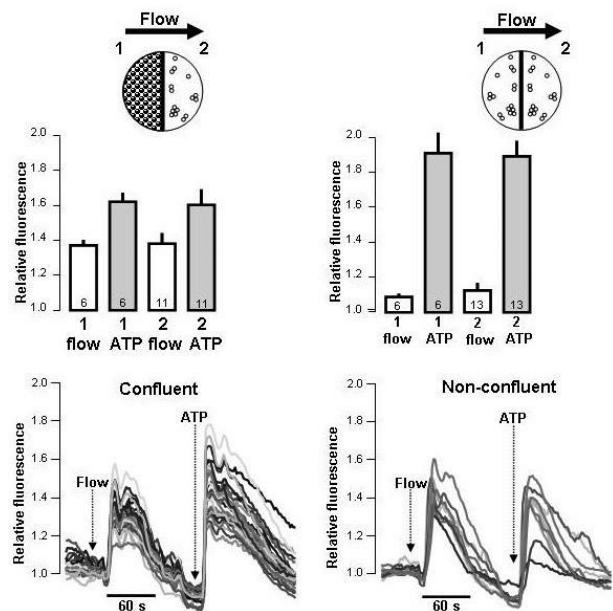
H. Praetorius and J. Leipziger

Institute for Physiology and Biophysics, University of Aarhus, Aarhus, Denmark

Cultured renal epithelial cells sense changes in fluid flow by their primary cilia (1). Freshly isolated renal tubules also respond changes in fluid flow by transient increases in the intracellular Ca^{2+} concentration, $[\text{Ca}^{2+}]_i$. The signal transduction pathway is, however, not well defined. Mechanical stimulation in general is known to promote release of nucleotides (ATP/UTP) and triggers auto- and paracrine activation of P2 receptors in renal epithelia. Recently, we showed that the flow-induced $[\text{Ca}^{2+}]_i$ response in freshly isolated medullary thick ascending limb (mTAL) involves mechanically stimulated nucleotide release (2). The flow/pressure induced response was

abolished by scavenging of ATP (apyrase) and by the un-selective P2-receptor antagonist (suramin). In addition, the flow/pressure induced response was strikingly lower in mice lacking the P2Y2 receptor, the predominant P2 receptor in mTAL. Our results strongly suggest that the flow-induced response is caused by release of bilateral nucleotides and subsequent activation of P2 receptors.

It is, however, not known if the primary cilium is necessary for this type of response. Here, we study the influence of extracellular nucleotides on the cilium dependent flow-response and address whether ATP is released during the course of the response. We used MDCK cells in a semi-open perfusion chamber model, where the flow response is known to be absolutely cilium-dependent at low flow rates. (A) We show that the epithelial sensitivity to changing flow rates is increased at low concentrations of nucleotides that do not by themselves induce $[\text{Ca}^{2+}]_i$ elevations. (B) Scavenging of ATP with apyrase (10U/ml) reduced the cilium-dependent flow response by 56.2%, whereas desensitisation of apical P2 receptors with ATP did not affect the response. (C) Non-ciliated MDCK cells, which do not respond to changes in fluid flow were used as reporter cells for paracrine ATP signalling. MDCK cells were grown on half coverslips and the non-confluent indicator cells were positioned on the out-flow side, directly next to the confluent cells. Intriguingly, the non-ciliated cells only responded to fluid flow with confluent ciliated cells on the inflow side (fig.). This was not the case if non-confluent, non-ciliated cells were placed on the inflow side. This paracrine response was reduced by scavenging of ATP. The data allow us to conclude that flow-induced, primary cilium-dependent $[\text{Ca}^{2+}]_i$ signalling is potentiated by stimulated nucleotide release.



Praetorius HA & Spring KR (2001). J Membr Biol 184, 71-79.

Jensen ME, Odgaard E, Christensen MH, Praetorius HA & Leipziger J (2007). J Am Soc Nephrol 18, 2062-2070.

Where applicable, the authors confirm that the experiments described here conform with The Physiological Society ethical requirements.

Where applicable, the authors confirm that the experiments described here conform with The Physiological Society ethical requirements.

C8

A range of functional consequences caused by Dent's disease missense mutations of ClC-5

A.J. Smith¹, A.A. Reed², N.Y. Loh², R.V. Thakker² and J.D. Lippiat¹

¹Institute of Membrane and Systems Biology, University of Leeds, Leeds, UK and ²Academic Endocrine Unit, University of Oxford, Oxford, UK

ClC-5 is a member of the voltage-gated chloride channel family that acts as a Cl⁻/H⁺ antiporter [1,2]. It is expressed in the proximal tubule of the kidney where it involved in small-peptide reabsorption from the urine. ClC-5 is predominantly located on endosomal membranes and has been proposed to provide a Cl⁻ conductance to counterbalance the action of v-ATPase. Mutation of ClC-5 has been linked to Dent's disease, an X-linked disorder characterised by proteinuria, hypercalciuria and nephrolithiasis [3].

We have examined the functional consequences of several known Dent's disease missense mutations. Data are expressed as mean \pm s.e.m., statistical significance determined by ANOVA. Following expression of wild-type (WT) and mutant EYFP-tagged ClC-5 in HEK293 cells, whole-cell currents were examined by patch-clamp electrophysiology. Current densities of cells expressing the G57V mutant (269 ± 30 pA/pF) were not different to WT (319 ± 45 pA/pF) ($p > 0.05$, $n = 5$) whereas R280P exhibited currents that were reduced by $\sim 50\%$ (155 ± 46 pA/pF) ($p < 0.05$; $n = 5$). Whole-cell currents of 5 other mutants (S270R, G513E, R516W, I524K & E527D) were not different to untransfected cells ($p < 0.05$; $n \geq 5$). Confocal imaging of cells showed that WT, G57V, R280P and E527D were located predominantly in intracellular endosomes and to varying extents at the cell surface. The four remaining mutants were retained in the endoplasmic reticulum. Endocytosis was examined in cells expressing WT and endosome-targeted mutant ClC-5. The uptake of fluorescently-conjugated albumin was increased ~ 5 -fold in cells expressing WT, G57V or R280P versus untransfected ($p < 0.01$; $n \geq 6$) but not in E527D expressing cells ($p > 0.05$; $n = 11$). Uptake of fluorescently-conjugated dextran and transferrin were not affected by the presence of ClC-5 ($p > 0.05$ vs untransfected; $n \geq 4$). Endosomal acidification was assayed using ratiometric pHluorin fused to VAMP2 for endosomal targeting [4]. Endosomes of untransfected cells bathed in pH 7.4 buffer were acidified to pH 6.98 ± 0.05 . Significant acidification was observed in cells expressing WT (pH 6.40 ± 0.17), G57V (pH 6.25 ± 0.19) and R280P (pH 5.46 ± 0.15) ($p < 0.01$ vs untransfected; $n \geq 15$ cells for each). Acidification in cells expressing E527D was impaired leading to a modest alkalinisation compared to untransfected cells (pH 7.55 ± 0.09) ($p < 0.05$; $n = 15$ cells).

These data suggest that Dent's disease does not necessarily result from a loss of a ClC-5 conductance from the endosome, but could be caused by disruption of another unidentified process involving ClC-5. They also suggest that efficient albumin endo-

cytosis requires functional ClC-5 at both surface and endosomal membranes.

Piccolo A & Pusch M (2005). *Nature*. **436**. 420-423

Scheel O, et al. (2005). *Nature*. **436**. 424-427

Lloyd SE, et al. (1996). *Nature*. **379**. 445-449

Miesenbock G, et al. (1998). *Nature*. **394**. 192-195

Supported by the Wellcome Trust

Where applicable, the authors confirm that the experiments described here conform with The Physiological Society ethical requirements.

C9

Role of WT1 in the regulation of expression of pro- and anti-angiogenic isoforms of VEGF

E. Amin^{1,2}, D.G. Nowak^{2,1}, S.J. Harper², D.O. Bates² and M.R. Ladomery¹

¹Centre for Research in Biomedicine, University of the West of England, Bristol, UK and ²Microvascular Research Laboratories, University of Bristol, Bristol, UK

The Wilms tumour suppressor gene WT1 is mutated in 10-15% of Wilms tumours and mutations in WT1 are also associated with Denys Drash Syndrome (DDS). DDS is characterised by childhood nephrotic syndrome, glomerulosclerosis, end-stage renal failure and Wilms tumours. WT1 encodes a zinc finger transcription factor that also regulates gene expression at the mRNA level. The search for WT1's DNA and mRNA targets is ongoing – a recent report has suggested that WT1 regulates the expression of a key growth factor, VEGF (Vascular Endothelial Growth Factor). There are two families of VEGF isoforms; an angiogenic family (VEGF_{xxx}); and a sister family of anti-angiogenic isoforms (VEGF_{xxx}b) that result from a distal alternative 3' splice site in exon 8 (Bates et al 2002). Although WT1 regulates VEGF expression transcriptionally, the extent to which WT1 affects VEGF isoform levels is not known, but splicing is altered in Denys Drash patients (Schumacher et al 2007). We measured VEGF isoform expression in differentiated wild-type and DDS patient-derived podocytes with a mutation in WT1 (R366C). The differentiated podocytes represents the closest in vivo model of podocytes in the kidney within the constraints of a cell culture model. Total VEGF and VEGF_{xxx}b levels were determined by ELISA and RT-PCR. In the differentiated DDS podocytes there was a 0.13 ± 0.002 fold reduction in the amount of VEGF_{xxx}b compared to wildtype differentiated podocytes while DDS stably transfected with wildtype WT1 restored the expression of VEGF_{xxx}b to 0.73 ± 0.08 . In the differentiated DDS podocytes there was a 2.32 ± 0.483 fold increase in the amount of panVEGF compared to wildtype differentiated podocytes. Transfection of the wildtype WT1 into the differentiated DDS podocytes manages to rescue the DDS phenotype by decreasing the amount of panVEGF to 0.618 ± 0.114 fold compare to wildtype podocytes. These results suggest that WT1 plays a role in the regulation of VEGF isoform expression; either by direct binding to VEGF pre-mRNA or by modulating splice factor activities

D.O. Bates, T-G. Cui, J.M. Doughty, M. Winkler, M. Sugiono, J.D. Shields, D. Peat, D.A. Gillatt, S.J. Harper. VEGF165b – an inhibitory splice variant of vascular endothelial growth factor is downregulated in renal cell carcinoma. *Cancer Research*. (2002) 62(14): 4123-31.

Schumacher VA, Jeruschke S, Eitner F, Becker JU, Pitschke G, Ince Y, Miner JH, Leuschner I, Engers R, Everding AS, Bulla M, Royer-Pokora B. *J Am Soc Nephrol*. 2007 18(3):719-29

Where applicable, the authors confirm that the experiments described here conform with The Physiological Society ethical requirements.

C10

Insulin directly remodels the glomerular filtration barrier of the kidney

R.J. Coward¹, G. Welsh^{1,4}, M. Bek², L. Hale¹, R. Lennon¹, H. Parvenstadt², S. Satchell¹, C. Caunt⁴, C. McCordle⁴, D. Griffiths³, J. Tavaré⁴, P. Mathieson¹ and M. Saleem¹

¹Academic Renal Unit, University of Bristol, Bristol, UK, ²Department of Medicine, University Clinics, Muenster, Germany, ³Department of Pathology, University hospital of Wales, Cardiff, UK and ⁴Department of Biochemistry, University of Bristol, Bristol, UK

Background:

Albuminuria is a cardinal sign of disruption to the glomerular filtration barrier (GFB), and it is the earliest marker of renal involvement in diabetes and the hyperinsulinaemic metabolic syndrome, which are conditions secondary to a failure of the production, or cellular action, of insulin.

Methods/findings:

We have studied the direct effect of insulin on the healthy glomerular filtration barrier using in vivo and in vitro techniques. In vivo- Wistar rats were treated with high physiological doses of insulin (1000pM) and their blood glucose levels maintained with a glucose infusion. These were compared to control animals given a saline infusion. Within 30 minutes insulin treated rats increased their urinary albumin excretion by 60% ($p < 0.01$). Animals were sacrificed and their kidneys perfused fixed. Insulin treated animals showed widening of their podocyte foot processes with less filtration slits per standardised unit length of filtration area ($p < 0.05$). There was also underlying swelling and vacuolation of endothelial cells. In vitro- Conditionally immortalised human glomerular podocyte and endothelial cell lines were examined. Human podocytes reorganised their actin cytoskeleton from stress fibre to cortical patterning within 15 minutes (phalloidin staining), with associated retraction of the fine processes of the cells (atomic force microscopy and real time imaging). Within 5 minutes, exclusively in podocytes, insulin switched on the small GTPase RhoA and switched off Rac1 and CDC42 (the molecular switches for actin reorganisation). Insulin also directly caused a functional loss of resistance across podocyte monolayers, but not endothelial cells (Electrical cell surface impedance sensing).

Conclusions:

Insulin has a previously unsuspected direct remodelling effect on the glomerular filtration barrier of the healthy kidney. As the earliest manifestation of renal involvement in diabetes and the metabolic syndrome is albuminuria, loss of mechanism could be of great importance and an early target for therapy.

Where applicable, the authors confirm that the experiments described here conform with The Physiological Society ethical requirements.

C11

A novel role for adiponectin in the glomerular filtration barrier?

F. Swan, J. Fabian, J.P. Shield, P.W. Mathieson, M.A. Saleem and G.I. Welsh

Academic Renal Unit, University of Bristol, Bristol, UK

In diabetic nephropathy, the most important cause of renal failure in the developed world, overt albuminuria is a marker for a poor prognosis not only from renal disease itself but also from associated cardiovascular disease[1-3]. How systemic disorders of insulin action lead to detrimental effects on the glomerular filtration barrier GFB is surprisingly poorly understood. There is accumulating evidence that the podocyte is central to the development of diabetic nephropathy, although the mechanism is not known[4]. We have recently reported the novel observation that human podocytes are insulin sensitive cells[5]. It is now recognised that adipocyte derived factors are important in regulating insulin sensitivity of distant tissues. The levels of one such factor, adiponectin, have been shown to be altered in end stage renal disease

This laboratory has developed and characterised in detail human conditionally immortalised podocyte and endothelial cell lines[6,7] We have been studying the effect of adiponectin on these cell lines. Using RTPCR and western blotting techniques we have found that podocytes, but not endothelial cells, produce adiponectin and secrete it into the media (Fig 1). This is surprising since this factor was thought to be solely produced by adipocytes. Like adipocytes, adiponectin production is regulated by insulin (Fig 2.). Immunofluorescence analysis demonstrates that the adiponectin is localized within the podocyte to intracellular vesicles. Both cell types express adiponectin receptors suggesting that they both respond to adiponectin. Using phosphospecific antibodies we are at present looking at the activation of various cell signalling pathways known to be activated in other cell types by adiponectin namely the Protein Kinase B, MAPK and AMPK pathways.

Conclusion: Our results, demonstrating surprisingly that podocytes produce and secrete adiponectin, a key regulator of insulin sensitivity and tissue inflammation [8], point to potential new mechanisms in the regulation of the physiology of the cells of the glomerular filtration barrier. Furthermore these results may point to a novel component in the pathogenetic mechanism of early diabetic nephropathy.

C13

Angiotensin-1 increases albumin reflection coefficient of isolated mouse glomeruli *ex vivo*

L. Sage, C.R. Neal, J.K. Ferguson, S.J. Harper, D.O. Bates and A.H. Salmon

Physiology, University of Bristol, Bristol, UK

Albuminuria represents excessive macromolecular permeability of the glomerular filtration barrier (GFB) and is a common feature of kidney disease. Angiotensin-1 (Ang1) is the only podocyte-produced molecule shown to reduce the reflection coefficient (σ) for albumin (σ_{alb}) of systemic microvessels¹. We hypothesised that Ang1 would decrease glomerular albumin permeability.

We previously described a refinement of a technique to measure water permeability (L_pA) in single isolated glomeruli, in which an oncotic pressure gradient drives fluid flux across the GFB, resulting in changes in glomerular volume². We have adapted this technique to measure glomerular σ_{alb} ³. σ describes the fraction of molecules retained by a membrane: for very large molecules that are perfectly retained by the GFB (e.g. >100kDa dextran), $\sigma = 1$; for albumin, σ of the GFB is just less than 1. A solution of albumin molecules will therefore exert a lower oncotic pressure across the GFB than an equivalent solution of dextran molecules. The ratio of these effective oncotic pressures is used to calculate σ_{alb} .

250kDa dextran was dialysed across a 100kDa membrane to eliminate smaller fragments that can cross the GFB. We created BSA and dextran solutions iso-oncotic to mouse plasma [$\pi=32.2\text{cm H}_2\text{O}$]⁴. Kidneys were extracted from humanely sacrificed Tie-2GFP mice. Glomeruli were isolated by flushing renal cortical tissue through graded metal sieves. Glomeruli were aspirated onto a micropipette within a flow-controlled observation chamber, then perfused with BSA and examined under static conditions for 2min. Perifusate was then switched to dextran. Glomerular volume during each perifusate incubation period (dextran: V_{dex} ; albumin: V_{alb}) was recorded on video, then calculated using ImageJ and Adobe Photoshop software. The ratio $V_{\text{dex}}/V_{\text{alb}}$ describes σ_{alb} .

Paired measurements of σ_{alb} were obtained in glomeruli before and after exposure to either 200ng/ml Ang1 or control solution for 1 hour. Whereas treatment of glomeruli with control solution did not alter σ_{alb} [from 0.9608 to 0.9639, $p>0.35$, paired t test, $n=15$], treatment with Ang1 significantly increased σ_{alb} [from 0.9725 to 0.9804, $p<0.05$, paired t test, $n=15$]. These results indicate a reduction in the macromolecular permeability of the GFB after treatment with Ang1 and support further research with Ang1 as a potential novel therapy in kidney disease.

Salmon AH *et al.* (2006). *Microcirc* **13**(6), 531.

Salmon AH *et al.* (2006). *J Physiol* **570**, 141-56.

Sage LM *et al.* (2007). *Microcirc* **14**(6), 653.

Stohrer M *et al.* (2000). *Cancer Res* **60**(15), 4251-5.

Supported by Kidney Research UK.

Where applicable, the authors confirm that the experiments described here conform with The Physiological Society ethical requirements.

C14

TRPC6 acts as a unique store calcium-release channel in podocytes, in a nephrin-dependent manner

R.R. Foster¹, M.A. Zadeh², G.I. Welsh¹, S.C. Satchell¹, P.W. Mathieson¹, D.O. Bates² and M.A. Saleem¹

¹Clinical Science @North Bristol, University of Bristol, Bristol, UK and ²Microvascular Research Laboratories, University of Bristol, Bristol, UK

Mutations in TRPC6 lead to increased intracellular calcium ($[\text{Ca}^{2+}]_i$) signalling and a phenotype of familial nephrotic syndrome, affecting the glomerular podocyte (1,2). In addition, in some acquired glomerulopathies increased podocyte TRPC6 expression is associated with the re-localisation, or downregulation of nephrin (3,4,5,6), a cell adhesion molecule and podocyte marker associated with the slit diaphragm. We sought to determine how podocytes are uniquely affected by TRPC6 mis-function and the role of nephrin using human conditionally immortalised podocytes (ciPods) and nephrin-deficient (ND) ciPods, previously characterised (7,8).

Cells were loaded with Fura2-AM, Methyl β cyclodextrin (M β CD), when used was added in the final 30mins of loading. Cells, incubated in Krebs' solution containing 1.5mM or 200nM Ca^{2+} , were stimulated with 200 μM flufenamic acid (FFA) in the presence or absence of thapsigargin (TG). $[\text{Ca}^{2+}]_i$ was proportional to the fluorescence intensity ratio (R_{norm}).

ciPods transfected with Ad-virus containing wild type and dominant negative TRPC6 constructs verified the specificity of FFA to TRPC6. 200 μM FFA increased the R_{norm} in ciPods in 1.5mM $[\text{Ca}^{2+}]_o$ (1.44 \pm 0.11 fold increase, $p\leq 0.01$ paired t-test) and surprisingly in 200nM $[\text{Ca}^{2+}]_o$ (1.58 \pm 0.01 fold increase, $P\leq 0.01$, paired t-test), but not after store-depletion (R_{norm} 1; 1.22 \pm 0.06 fold increase) in contrast to an increase in ND ciPods after store-depletion (1.6 \pm 0.06 fold increase, $p\leq 0.05$, paired t-test). Pre-incubation of ciPods with 1mM M β CD inhibited the response to FFA in 1.5mM $[\text{Ca}^{2+}]_o$ as expected (R_{norm} 1.07 \pm 0.03 fold increase), yet also blocked the response in 200nM $[\text{Ca}^{2+}]_o$ (R_{norm} 1.19 \pm 0.01 fold increase), verifying TRPC6 function as a store calcium release channel.

In conclusion, FFA specifically activates TRPC6 in ciPods. In these cells TRPC6 can uniquely act as a store calcium-release channel, although only in the presence of nephrin. The activation of TRPC6 is lipid raft dependent, whether in the plasma membrane or on internal stores.

Winn MP *et al.* (2005). *Science* 308:1801-1804.

Reiser J *et al.* (2005). *Nat Genet* 37:739-744.

Moller CC *et al.* (2007). *J Am Soc Nephrol* 18:29-36.

Doublier S *et al.* (2001). *Am J Pathol* 158:1723-1731.

Kim BK *et al.* (2002). *Am J Kidney Dis* 40:964-973.

Coward RJ *et al.* (2005) *J Am Soc Nephrol* 16:629-637.

Saleem MA *et al.* (2002). *J Am Soc Nephrol* 13:630-638.

Foster RR *et al.* (2005). *Am J Physiol Renal Physiol* 288:F48-57.

This project was funded by the MRC.

Where applicable, the authors confirm that the experiments described here conform with The Physiological Society ethical requirements.

C15

The effect of hypertension on the filtration barrier of subpodocyte spaces in rat glomerular capillaries

C.R. Neal, V.J. Murdin, P.R. Muston, D.O. Bates and S.J. Harper

Microvascular Research Labs, Physiology Dept, University of Bristol, Bristol, UK

Bowman's space consists of three interconnected urinary spaces forming drainage pathways for ultrafiltrate (Neal CR *et al.* 2005, 2007). Glomerular filtrate may enter restrictive urinary spaces under the podocyte cell body (subpodocyte space, SPS) before passing to other urinary spaces. We have measured SPS in 12 week old (early) spontaneously hypertensive rats (SHR) or Wistar Kyoto rats (WKY) controls after fixation at physiological oncotic and hydrostatic pressures.

SHR (mean arterial pressure (MAP) 140mmHg) or WKY (MAP 96mmHg) kidneys from pentobarbital (i.p.) euthanased rats were perfusion fixed at matched MAP with isoncotic glutaraldehyde solutions. Serial ultrathin sections of kidney were used to reconstruct regions of glomeruli. From these filtration slit density of the glomerular capillary wall, SPS coverage of the capillaries, and the available area for filtration into the SPS was measured and compared (mean \pm SEM, unpaired t-test).

The filtration slit density along the glomerular filtration barrier in non-SPS regions of the SHR and WKY was the same (2.3 \pm 0.2 per μ m, n=14, 2.3 \pm 0.1 per μ m, n=15). However, filtration slit density decreased in the covered SPS regions of SHR glomerular capillaries (1.8 \pm 0.1 per μ m, n=14, P <0.05) compared with WKY controls (2.1 \pm 0.1 per μ m, n=15). The SPS covered area of the glomerular filtration barrier was similar in both (62 \pm 14% to 72 \pm 9%).

Mild hypertension in 12 week old SHR produces a decrease in the number of filtration slits of the filtration barrier covered by SPS. This reduction in filtration pores suggests a lower permeability in these SPS covered regions compared to uncovered regions (non-SPS).

Neal CR *et al.* (2005). *J Am Soc Nephrol* 16, 1223-35.

Neal CR *et al.* (2007). *Am J Physiol Renal Physiol* Sep 5; (Epub ahead of print).

Where applicable, the authors confirm that the experiments described here conform with The Physiological Society ethical requirements.

C16

Podocyte specific over-expression of VEGF-A₁₆₅b significantly reduced the normalised ultrafiltration coefficient in the absence of any change in reflection coefficient

J.K. Ferguson, Y. Qiu, L.M. Sage, C.R. Neal, D.O. Bates, S.J. Harper and A.H. Salmon

Physiology (MVRL), University of Bristol, Bristol, UK

The glomerular filtration barrier (GFB) has three main cellular components: fenestrated endothelial cells; basement membrane; and podocyte foot processes. In health the GFB is highly permeable to water and small solutes but almost entirely impermeable to proteins. Vascular endothelial growth factor A (VEGF-A) is produced by podocytes. Tight regulation of VEGF-A expression is critical for the establishment and maintenance of the GFB¹, and glomerular VEGF expression is disrupted in many glomerular diseases². Differential splicing of the VEGF-A gene forms two families of isoforms: the pro-angiogenic family (VEGF-A_{xxx}), and the anti-angiogenic families (VEGF-A_{xxx}b). VEGF-A₁₆₅ contributes to the high permeability of glomeruli to water³. We sought to determine the effects of VEGF-A₁₆₅b on glomerular permeability by examining permeability coefficients in glomeruli harvested from transgenic mice with podocyte specific heterozygosity (^{+/+}) for VEGF-A₁₆₅b. The water permeability of isolated mouse glomeruli (normalised ultrafiltration co-efficient: $L_p A/V_i$) was assessed using a previously described oncometric technique³. $L_p A/V_i$ is calculated from the rate of change of glomerular volume after introduction of an oncotic pressure gradient of known magnitude. VEGF-A₁₆₅b over-expression reduced glomerular $L_p A/V_i$ as compared with wild-type littermate controls (VEGF-A₁₆₅b^{+/+}: 1.44 \pm 0.11, n=18; controls: 1.93 \pm 0.16, n=8; unpaired t-test: p =0.017).

We have modified this methodology to estimate the reflection coefficient to albumin (σ_{alb})⁴. The volume of a glomerulus incubated in dextran solution, expressed as a fraction of the volume of the same glomerulus when incubated in an iso-oncotic solution of albumin, describes σ_{alb} . Compared with wild-type littermate controls, there was no significant difference in the σ_{alb} in glomeruli harvested from VEGF-A₁₆₅b^{+/+} mice (VEGF-A₁₆₅b^{+/+}: 0.975 \pm 0.011, n=9; controls: 0.998 \pm 0.02, n=11; unpaired t-test p =0.32).

These results suggest that a higher concentration of podocyte VEGF-A₁₆₅b does not reduce the ability of the barrier to retain macromolecules. Altering the balance of VEGF-A_{xxx} and VEGF-A_{xxx}b in disease states may be of therapeutic interest.

Eremina V *et al.* (2003). *J Clin Invest* 111, 707-716.

Schrijvers KI *et al.* (2004). *Kidney Int* 65 (6), 2003-2017.

Salmon AH *et al.* (2006). *J Physiol* 570, 141-56.

Sage LM *et al.* (2007). *BMS Spring Meeting*, Belfast.

Supported by the British Heart Foundation.

Where applicable, the authors confirm that the experiments described here conform with The Physiological Society ethical requirements.

PC1

The revertant mutants G550E and 4RK alter the processing efficiency and gating behaviour of G551D-CFTR

Z. Xu¹, L.S. Pissarra^{2,3}, C.M. Farinha^{2,3}, D.N. Sheppard¹ and M.D. Amaral^{2,3}

¹Dept. Physiol. & Pharm., University of Bristol, Bristol, UK, ²Dept. Chem. & Biochem., University of Lisboa, Lisboa, Portugal and ³Centre of Human Genetics, National Institute of Health, Lisboa, Portugal

The simultaneous mutations of four arginine-framed tripeptides (AFTs) (R29K, R516K, R555K and R766K; 4RK) in cystic fibrosis transmembrane conductance regulator (CFTR) rescues the processing and function of the most common cystic fibrosis mutation, F508del [1]. G550E, another F508del revertant, exerts, by itself, a similar effect [2]. Recently, we demonstrated that 4RK affects mainly processing efficiency, whereas G550E appears to act directly on CFTR structure, as it rescues efficaciously F508del gating [3]. Of note, the G550E revertant is located next to G551, the site of a CF mutant (G551D) that profoundly disrupts CFTR gating. Here, we explore the effects of G550E and 4RK on the processing and gating of G551D. We used BHK cells expressing G551D-, G551D-G550E- and G551D-4RK-CFTRs, metabolic pulse-chase labelling to study protein processing and excised inside-out membrane patches to examine channel gating [3]. Data are means \pm SEM of *n* observations; statistical analyses were performed using Student's paired *t* test.

Unlike F508del, G551D is processed normally. However, the processing efficiency of G551D was modulated by revertant mutants with G550E, but not 4RK, increasing processing efficiency. These data contrast with the effects of the revertants on wild-type (wt) and V562I, where 4RK, but not G550E, enhanced processing efficiency [3]. In contrast to wt, the inter-burst interval (IBI) of G551D was prolonged greatly and the mean burst duration (MBD) reduced with the result that P_o was diminished markedly (wt, $P_o = 0.47 \pm 0.03$, *n* = 7; G551D, $P_o = 0.007 \pm 0.001$, *n* = 8). Although both G550E and 4RK increased the P_o of G551D, they were ineffective at rescuing channel activity. Surprisingly, while both revertants attenuated markedly IBI, they also shortened MBD (G551D-G550E, $P_o = 0.010 \pm 0.001$, MBD = 27 ± 4 ms, IBI = $2,772 \pm 301$ ms, *n* = 13 for all; G551D-4RK, $P_o = 0.027 \pm 0.005$, MBD = 11 ± 1 ms, IBI = 535 ± 113 ms, *n* = 14 for all; *p* < 0.05). As a result, the gating behaviour of G551D-G550E and G551D-4RK appeared very flickery.

To summarise, the revertant G550E increased the processing of G551D, but not that of wt and V562I [3], whereas, both G550E and 4RK restored function to F508del [3], but not G551D. Our data suggest that when in cis with G551D, AFTs might influence directly channel gating, arguing that 4RK, in addition to its effects on trafficking, might alter G551D folding. Thus, the effects of G550E and 4RK on protein processing and channel gating are mutation-specific.

Chang X-B et al. (1999). *Molecular Cell* 4, 137-142.

DeCarvalho AC et al. (2002). *J Biol Chem* 277, 35896-35905.

Roxo-Rosa M et al. (2006). *Proc Natl Acad Sci USA* 103, 17891-17896.

Supported by CF Trust (UK) and FCT (Portugal). ZX is supported by an ORS award and a University of Bristol Scholarship.

Where applicable, the authors confirm that the experiments described here conform with The Physiological Society ethical requirements.

PC2

Effects of the KCNQ1 K⁺ channel inhibitor chromanol 293B on renal function in wildtype and KCNE1 knockout mice

A. Neal¹, J. Kibble³, S. White² and L. Robson¹

¹Biomedical Science, University of Sheffield, Sheffield, South Yorkshire, UK, ²Institute of Membrane and Systems Biology, University of Leeds, Leeds, West Yorkshire, UK and ³Medicine, Memorial University Newfoundland, St. John's, NF, Canada

The K⁺ channel β subunit KCNE1 plays a role in proximal tubule function, maintaining electrogenic transport. KCNE1 knockout (KO) mice show increased urinary excretion of Na⁺, glucose and fluid (Vallon, 2001). KCNE1 regulates KCNQ1, which is found in the kidney. However, the renal response in KCNQ1 KO mice is different (Vallon, 2005). In addition, a recent report indicated a distal location for KCNQ1 (Zheng, 2007). The aim of this study was to examine the renal response to chromanol 293B, a KCNQ1 inhibitor, comparing responses in wildtype (WT) and KCNE1 KO mice. Adult WT and KCNE1 KO mice were anaesthetised initially with Na⁺ thiopentone (100 mg/kg) and anaesthesia maintained with ketamine (10mg/kg) and xylazine (1.5 mg/kg), all intra peritoneal injections. They were then surgically prepared for renal clearance measurements. Animals received an intravenous infusion of 2.25g/dl BSA in isotonic saline. After surgery, chromanol 293B (12 μ mol/kg/hr) or clofilium (K⁺ channel inhibitor, 9 μ mol/kg/hr) were administered. After 45 minutes equilibration urine was collected over 60 minutes. 3H-inulin was infused to allow determination of GFR. Controls received an equivalent dose of vehicle (DMSO). At the end of the collection period, a terminal blood sample was taken to obtain plasma. Statistical significance was assessed using ANOVAs and treatment tests, with significance assumed at the 5% level. Knock-out of KCNE1 increased urine flow and the fractional excretion (FE) of Na⁺ and Cl⁻ (Table 1). The FE_{glucose} was unaffected in KO animals, $0.30 \pm 0.06\%$ versus $0.26 \pm 0.06\%$ in WT and KO, respectively. Infusion of chromanol 293B in WT mice mimicked the response observed in KO animals, while chromanol was without effect in KO mice. In contrast, clofilium increased the FE of Na⁺ and Cl⁻ in WT and KO animals. There was no effect on urine flow, probably due to a reduced GFR in the clofilium treated mice. These data indicate that KCNE1 regulates a chromanol 293B sensitive K⁺ channel in renal tubules. Given the previous work on KCNE1, the location of this channel is likely to be the proximal tubule, although further work is needed to confirm both channel location and identity.

Table 1: Renal parameters in WT and KO mice

	WT (n=8)	WT chromanol (n=6)	WT clofilium (n=10)	KO (n=9)	KO chromanol (n=9)	KO clofilium (n=9)
GFR ($\mu\text{l}/\text{min}$)	480 \pm 44.7	402 \pm 16.5	279 \pm 18.3*	423 \pm 31.6	393 \pm 17.9	267 \pm 17.2#
Urine flow ($\mu\text{l}/\text{min}$)	8.7 \pm 1.1	14.9 \pm 1.1*	8.4 \pm 0.8	12.2 \pm 1.4*	11.8 \pm 1.0	10.6 \pm 0.8
FENa ⁺ (%)	2.1 \pm 0.3	4.2 \pm 0.2*	3.9 \pm 0.4*	3.3 \pm 0.4*	3.8 \pm 0.4	4.7 \pm 0.4#
FECl ⁻ (%)	3.3 \pm 0.5	5.8 \pm 0.4*	5.2 \pm 0.5*	4.7 \pm 0.6*	5.1 \pm 0.5	6.5 \pm 0.5#

* indicates a significant difference to WT. # indicates a significant difference to KO

Vallon et al. 2001. Role of KCNE1-dependent K⁺ fluxes in mouse proximal tubule. *J Am Soc Nephrol* 12, 2003–2011.

Vallon et al. 2005. KCNQ1-dependent transport in renal and gastrointestinal epithelia. *PNAS* 102, 17864–17869.

Zheng et al. 2007. Cellular distribution of the potassium channel KCNQ1 in normal mouse kidney. *Am J Physiol Renal Physiol* 292, F456–F466.

This work was supported by the Wellcome Trust.

Where applicable, the authors confirm that the experiments described here conform with The Physiological Society ethical requirements.

PC3

Synthesis of basement membrane by cultured human glomerular cells

S. Slater, M. Saleem, P. Mathieson and S. Satchell

Academic Renal Unit, Bristol University, Bristol, UK

In vivo the glomerular basement membrane is a specialised structure consisting of heparan sulphate proteoglycans (HSPG) and particular isoforms of collagen type IV and laminin. Currently there is controversy as to whether podocytes or glomerular endothelial cells (GEnC), or a combination of both, produce this matrix. We studied basement membrane production using conditionally immortalised human GEnC and podocyte cell lines. Both whole cell lysates and isolated basement membrane from conditionally immortalised cells in either the proliferating or differentiated state were analysed. Cells were removed from flasks or coverslips after incubation for 1 week, using 1% Triton containing 20mM ammonium hydroxide. This left behind basement membrane which was examined using immunofluorescence (IF) for pan collagen type IV, collagen IV α 1, α 2, α 3 and α 5 chains, heparan sulphate and binding of wheat germ agglutinin (lectin). The reactivity of the antibodies against glomerular basement membrane was confirmed by IF on tissue sections. The ability of cells to grow on matrix produced by cells was examined by light microscopy and IF for VE-cadherin. Cell and matrix lysates were further analysed by Western blotting for specific α chains of collagen type IV.

IF (n=2) showed pan collagen type IV, collagen IV α 1 and glycoproteins, including HSPG were produced by both cell types. Collagen IV α 3 and α 5 chains were detectable in proliferating and differentiated cells by Western blotting (n=3). Collagen IV α 5 chains were only detectable in podocyte lysates, whereas α 3 chains were present in both GEnC and podocytes lysates. Seed-

ing GEnC onto podocyte produced matrix resulted in the cells growing normally, and vice versa.

In summary, in vitro both cell types produce components of the specialised glomerular basement membrane which cells will grow on. Future work will focus on further analysis of the specific isoforms of collagen type IV produced by these cells, and also the rate at which these cells attach to matrix.

Where applicable, the authors confirm that the experiments described here conform with The Physiological Society ethical requirements.

PC5

Imaging of mitochondrial function in live slices of rat kidney by multi-photon microscopy

A.M. Hall, R.J. Unwin and M.R. Duchon

Physiology, UCL, London, UK

Different segments of the nephron appear to be differentially sensitive to mitochondrial cytopathy; clinically the proximal tubule (PT) appears particularly vulnerable, and dysfunction of the PT can lead to the renal Fanconi syndrome (1). We have developed a method, using multi-photon microscopy (2), to investigate underlying differences in mitochondrial function between the PT and other nephron segments in live rat kidney tissue, which might explain this clinical observation.

Adult male Sprague-Dawley rats were killed humanely and their kidneys were immediately removed and placed into ice-cold Krebs solution gassed with oxygen.

Live 200 μm slices of kidney were produced using a Microm 650V tissue slicer. The slices were imaged with a Zeiss LSM 510 upright multi-photon microscope, coupled with a Coherent Chameleon tunable laser. An onstage perfusion system was used to infuse metabolic substrates, dyes and mitochondrial reagents; thus allowing changes in mitochondrial function in different cell types to be imaged in real time.

We have found that renal tubular cells emit a large background auto-fluorescence signal when excited at a range of wavelengths from 720–850nm. With excitation at 720nm, the blue fluorescence emitted is predominantly mitochondrial NADH. Green fluorescence arises partly from oxidized flavoproteins. The identity of the signal can be confirmed by a change in response to either respiratory chain inhibitors or uncoupling agents. Different parts of the tubule can be distinguished by their auto-fluorescence signals. Calcein labels living cells, confirming viability, and is also useful to identify structures.

Tetramethyl rhodamine methyl ester (TMRM) is used to visualize variations in mitochondrial location, potential difference and morphology in different cell types (3). TMRM signal is brighter in more distal parts of the tubule compared with the PT, suggesting that mitochondria in these regions may be more polarized.

Multi-photon imaging of live slices of rat kidney is a useful technique to investigate mitochondrial function in the kidney. It allows direct comparison of different nephron segments in primary, non-immortalized tissue, with preserved architecture. Furthermore, it permits access to structures that are difficult to visualise in the whole intact organ. Early results suggest differences

between the PT and other nephron segments, which may prove to be important in the nature and localization of renal cell injury.

1. Martin-Hernandez E et al. (2005). *Pediatr Nephrol* 20:1299-1305.
2. Sipos A et al. (2007). *Kidney Int Aug* 1.
3. Duchen MR et al. (2003). *Methods Enzymol* 361, 353-89.

Where applicable, the authors confirm that the experiments described here conform with The Physiological Society ethical requirements.

PC6

Use of REFER analysis to map the gating pathway of the human CFTR Cl⁻ channel

Z. Cai and D.N. Sheppard

Department of Physiology and Pharmacology, Bristol University, Bristol, UK

The cystic fibrosis transmembrane conductance regulator (CFTR) is a Cl⁻ channel gated by ATP-driven nucleotide-binding domain (NBD) dimerisation. To investigate the gating pathway of CFTR, we performed rate-equilibrium free energy relationships (REFER) measurements (1, 2). We used site-directed mutations as structural probes, and ATP and voltage as environmental probes of channel gating (1) and C1 \leftrightarrow C2 \leftrightarrow O scheme to describe CFTR channel gating (3). C1 represents the long duration closed state separating channel openings and C2 \leftrightarrow O the bursting state. Transitions between C1 \leftrightarrow C2 and C2 \leftrightarrow O are described by the forward rate constants β_1 and β_2 and the backward rate constants α_1 and α_2 , respectively. As CFTR is gated by intracellular ATP, C1 \leftrightarrow C2 reflects agonist binding step, whereas C2 \leftrightarrow O reflects the gating step (4). REFER analysis is applied to the gating step. β_2 and α_2 are used to generate a Brønsted plot (log (β_2) plotted vs. log (β_2/α_2)). The slope of the line in a Brønsted plot (Φ) quantifies the relative extent to which the opening (β_2) and closing (α_2) rate constants change and provides an estimate of the temporal sequence of intermediate events during channel gating. Φ ranges between 0 and 1. When Φ is close to 1, the transition-state resembles an open-channel conformation and moves early during gating, whereas when Φ is close to 0, the transition-state resembles a closed-channel conformation and moves late during gating (1, 2).

Brønsted plots of mutations (G550E, G551D, V562I, G551D-G550E, V562I-G550E) in the H5 α -helix of NBD1 ($n = 3-14$), different ATP concentrations (0.03–5 mM, $n = 8-33$) and a membrane voltage series (-100 – +100 mV, $n = 5-7$) yielded Φ values of 0.64 ($r^2 = 0.91$), 0.84 ($r^2 = 0.55$) and 0.18 ($r^2 = 0.71$), respectively. Good linear fits of the Brønsted plots of these perturbations indicate that CFTR is amenable to REFER analysis. We interpret our data to suggest that at the transition state, i) the structure of the H5 α -helix is a hybrid, which is more open than closed; ii) the ATP-binding sites are almost completely in the open state, arguing that the conformations of the ATP-binding sites change early in the CFTR gating pathway; iii) the CFTR pore is almost closed at the transition state, suggesting that the conformation of the CFTR pore changes late in the CFTR gating pathway. We conclude that there is a spatial gradient of Φ val-

ues from ~ 0.90 at the ATP-binding sites to ~ 0.20 at the CFTR pore. Thus, as proposed by Grosman *et al* (1), initiation at the effector site and propagation to the active site is likely to be a common theme for the gating of ion channels activated by ligands.

Grosman C *et al.* (2000). *Nature* 403, 773-776.

Purohit P *et al.* (2007). *Nature* 446, 930-933.

Winter MC *et al.* (1994). *Biophys J* 66, 1398-1403.

Colquhoun D (1998). *Br J Pharmacol* 125, 923-947.

We thank LS Pissarra and MD Amaral for the generous gift of CFTR constructs and Z Xu for excellent assistance. This work was supported by the BBSRC and CF Trust.

Where applicable, the authors confirm that the experiments described here conform with The Physiological Society ethical requirements.

PC7

Membrane depolarisation indirectly regulates the Ca²⁺-activated Cl⁻ conductance in mouse renal inner medullary collecting duct cells (mIMCD-3)

S.H. Boese¹, J.E. Linley³, M.A. Gray² and N.L. Simmons²

¹Zoophysiology, University of Potsdam, Potsdam, Germany,

²Institute for Cell & Molecular Biosciences, Newcastle University, Newcastle upon Tyne, UK and ³Institute of Membrane & Systems Biology, University of Leeds, Leeds, UK

Renal inner medullary collecting duct cells (mIMCD-3) possess a Cl⁻ conductance (CaCC) regulated by intracellular Ca²⁺ via Ca²⁺ influx across the apical plasma membrane (Stewart *et al*, 2001). Tpc1 is a Ca²⁺ permeable channel activated by depolarisation which is expressed in mIMCD-3 cells (Sayer *et al*, 2006) but whose physiological role is undefined.

Here we investigate the effect of membrane depolarisation on CaCC in mIMCD-3 cells. Membrane conductance of cells on coverslips was measured using the slow whole cell patch-clamp technique. Data are given as mean \pm SEM (n), difference between mean values was determined by Student's *t* test.

When the membrane potential was held at -60mV (V_{hold}) with brief excursions to +60mV, only a small basal K⁺ conductance was detected. In contrast, when V_{hold} was 0mV with brief excursions to ± 60 mV, there was a slow increase in conductance following a delay of ~ 60 s. Whole cell conductance increased from 30.7 ± 3 & -18.4 ± 2 pA/pF (at $V_{\text{hold}} = -60$ mV) to 214.4 ± 22 & -108.9 ± 9 pA/pF (at $V_{\text{hold}} = 0$ mV) ($n = 37$) reaching a plateau after ~ 15 mins ($T_{0.5} = 472 \pm 23$ s). Currents were outwardly-rectifying, time-independent and Cl⁻ selective. Repolarisation ($V_{\text{hold}} = -60$ mV), reversed the conductance increase to control values ($T_{0.5} = 90 \pm 10$ s, $n=15$).

The sensitivity to depolarisation and dependence on Ca²⁺ influx suggests the involvement of a tpc1 like channel in CaCC activation. A distinguishing feature of tpc1 is its Al³⁺ sensitivity (Kawano *et al*, 2004). Whereas 1mM Al³⁺ did not effect basal conductance at -60mV, the activation of CaCC was abolished by 1mM Al³⁺ when V_{hold} was 0mV. The effect of 1mM Al³⁺ was com-

pletely reversible on washout of Al^{3+} with V_{hold} at 0mV but subsequent activation of CaCC was ~four fold faster. Finally, 1mM Al^{3+} failed to inhibit the pre-activated Cl^- conductance at 0mV. Taken together these data indicate that Al^{3+} blocks the depolarisation-induced activation of CaCC, but Al^{3+} has no direct blocking effect on the activated Cl^- conductance itself. This suggests that the physiological role of tpc1 is to act as the voltage-sensor upon membrane depolarisation to regulate CaCC in the apical membrane of IMCD cells.

Kawano T, Kadano T, Fumoto K, Lapeyrie F, Kuse M, Osobe M, Furuichi T, Muto S (2004). *Biochem Biophys Res Comm* 324, 40-45.

Sayer JA, Carr G, Morgan EL, Kellett GL, Simmons NL (2006). *Proc Physiol Soc* 2, PC22.

Stewart GS, Glanville M, Aziz O, Simmons NL Gray MA (2001). *J Membrane Biol* 180, 49-64.

Supported by Kidney Research UK.

Where applicable, the authors confirm that the experiments described here conform with The Physiological Society ethical requirements.

PC8

A comparison of P2 receptor mRNA expression levels in the renal collecting duct in response to altered dietary sodium and in DOCA-induced hypertension

L. Yew-Booth², M. Le Bras², S. Balesaria², J. Marks², C.M. Turner², D.G. Shirley², R.J. Unwin² and S.S. Wildman^{1,2}

¹Veterinary Basic Sciences, Royal Veterinary College, London, UK and ²Physiology, Nephrology and Biochemistry, UCL, London, UK

The epithelial Na^+ channel (ENaC) is a regulated pathway for Na^+ uptake across the luminal membrane of the renal collecting duct (CD) and plays an important role in blood pressure control. Activation of many P2 receptor (P2R) subtypes (including: $\text{P2X}_{2,4,2/6}$ and/or $4/6$ and P2Y_{2} and/or 4) expressed in CD epithelial cells can alter ENaC activity in different ways (Wildman *et al.* 2005, 2007). It is known that changes in ENaC activity - when co-expressed in *Xenopus* oocytes or following dietary Na^+ restriction in native CD tissue - affects the expression levels of some P2Rs ($\text{P2X}_{1,2,4,5}$ and 6 subunits and P2Y_4) (Wildman *et al.* 2005; 2007). We have proposed that P2Rs may locally regulate ENaC activity in the CD and that some P2Rs could be involved in the pathogenesis of hypertension. To examine the relationship between P2Rs and ENaC in the CD we have investigated P2R mRNA levels in CDs from adult Sprague-Dawley rats maintained on 'low' (0.01%), 'normal' (0.5%) or 'high' (4%) Na^+ diets (10 days) to alter ENaC expression and activity, and in DOCA-salt hypertensive rats (unilateral nephrectomy and DOCA treatment for 5 weeks; $\text{SBP} = 189 \pm 12 \text{ mmHg}^{-1}$, $n = 6$). Kidneys from terminally anaesthetized rats were microdissected and CDs isolated (~15 mm; $n = 6$ for each sample). RNA was extracted and reverse transcribed, and the cDNA transcripts used for real time-PCR. A ratio was calculated of the P2R gene of interest (either $\text{P2X}_{1,7}$ or $\text{P2Y}_{1,2,4}$ and 6) to a constitutively expressed house-keeping gene (HPRT). We could not detect significant levels (i.e. >0.5 arbitrary units; AU) of $\text{P2X}_{2,3,5,7}$ and P2Y_1 mRNA under any experimental condition

($n = 6$). In contrast, significant amounts of mRNA (1-2 AU) were detected for P2X_4 and P2Y_{2} and 6 in CDs from rats on a 'normal' Na^+ intake. CDs from rats on a 'low' Na^+ diet showed a significant increase in abundance of P2X_4 and P2Y_6 mRNA (by 2-fold; $n = 6$, $P < 0.01$); CDs from rats maintained on a 'high' Na^+ diet showed a significant decrease in abundance of P2Y_2 mRNA (to less than 0.5 AU; $n = 6$); CD P2X_{1} and 6 and P2Y_4 mRNA levels were not significant on a 'normal' Na^+ diet, but were increased on a 'low' Na^+ diet ($n = 6$). However, there were no differences in mRNA expression between 'normal' Na^+ diet and hypertensive rats ($n = 6$). Thus, P2R mRNA expression levels change in the rat CD in response to changes in dietary Na^+ , but not in DOCA-salt hypertensive rats. From these data it is unlikely that altered CD P2R function plays a role in this model of hypertension.

Wildman SS *et al.* (2005). *J Am Soc Nephrol* 16, 2586-2597.

Wildman SS *et al.* (2007). *FASEB* 21(6), A1328.

Supported by Wellcome Trust, British Heart Foundation and St Peter's Trust.

Where applicable, the authors confirm that the experiments described here conform with The Physiological Society ethical requirements.

PC9

Rhesus associated glycoproteins, RhBG and RhCG; investigating localisation and interactions in the kidney

A.C. Brown, S. Ashman and A.M. Toye

Biochemistry, University of Bristol, Bristol, UK

In healthy individuals excess acid generated from metabolism is excreted into the urine by specialised alpha-Intercalated cells (α -IC) of the distal tubule. These cells require the co-ordinated action of several proteins to adequately acidify the urine. One such protein, located at the blood-facing surface (the basolateral membrane) of the α -IC, is kidney anion exchanger 1 (kAE1), a truncated isoform of the red blood cell anion exchanger 1 (eAE1, Band 3). Specific mutations of the AE1 gene cause distal renal tubular acidosis (dRTA) demonstrating its essential role in urine acidification. We are interested in characterising interactions between kAE1 and other proteins that may play a role in regulating kAE1 trafficking or stabilise it at its basolateral membrane location. In the erythrocyte AE1 is known to be a fundamental component of an AE1-Rh membrane protein macrocomplex, which includes the Rhesus associated protein, RhAG. Importantly, the α -IC contains two RhAG homologues, RhBG and RhCG, that are thought to be implicated in acid secretion via ammonia transport. We have created novel RhBG and RhCG cell lines and antibodies to test our hypothesis that a similar RhBG or RhCG:kAE1 complex may exist in the kidney.

To independently confirm the location of RhBG and RhCG in the kidney we have created and polarised MDCKI cell lines stably expressing either human RhBG or RhCG tagged with C- or N-terminal GFP in the presence and absence of kAE1. We have shown that choice of location of the GFP tag on RhBG or RhCG can influence the polarised localisation of the proteins. The cell lines, and human kidney tissue, have been used to characterise

novel antibodies to RhCG that are now being used to investigate RhCG distribution and putative *in vivo* kAE1 co-localisation in human and mouse kidney. We are now utilising these novel cell lines to investigate the existence of a putative RhBG or RhCG:kAE1 interaction in the basolateral membrane. This cell model system will also allow for future investigation to define the physiological function of these transporters.

This work is funded by a Kidney Research UK and Glaxo-SmithKline PhD studentship and a NHS Blood and Transplant Wellcome Trust Fellowship.

Where applicable, the authors confirm that the experiments described here conform with The Physiological Society ethical requirements.

PC10

High dietary sodium intake - an oxidative stress for the kidney?

E.J. Johns, B. O'Shaugnessy, S. O'Neill, B. Lane and V. Healy

Department of Physiology, University College Cork, Cork, Ireland

Mitochondrial respiration by the enzymes NAD(P)H, xanthine oxidase and others results in the production of reactive oxygen species (ROS) which comprise superoxide anions (O₂⁻), hydroxyl radicals (OH⁻) and hydrogen peroxide (H₂O₂). These species can damage other cellular proteins and degrade nitric oxide (NO) but their action is limited by the scavenging enzyme superoxide dismutase (SOD). In pathophysiological states, such as hypertension, heart failure, obesity and diabetes ROS production is increased reflecting a state of oxidative stress (Wilcox, 2002). What is less clear is how physiological challenges to cardiovascular and renal function may impact on ROS production. This was investigated by examining how the levels of enzymes involved with ROS generation in the renal cortex and medulla responded to a period of elevated dietary sodium intake.

Male Wistar rats, 225-275g, were maintained on either a normal (0.3% Na) or a high salt diet (3% Na) for two weeks. Groups of 6-8 rats were placed in metabolic cages before and one and two weeks after dietary manipulation for 24h urine collections to allow estimation of fractional sodium and 8-isoprostane excretion. At the end of this period they were sacrificed, kidneys removed and separated into cortex and medulla/papilla, homogenized and proteins extracted. SOD and NAD(P)H expression and activity were measured. Data, means \pm SEM, were analysed using Student's 't' test and significance taken at $P < 0.05$.

After two weeks high sodium, fractional sodium excretion increased from 1.0 ± 0.2 to 21 ± 5 and 8-isoprostane excretion from 10 ± 2 to 120 ± 30 pg/kg/h (both $P < 0.001$). NAD(P)H oxidase activity and protein expression increased some two-fold (both $P < 0.05$) in the cortex, but not medulla in the rats subjected to the high salt diet. SOD activity was higher in the medulla than cortex in normal and high salt diet rats (both $P < 0.05$). Protein expression of copper and zinc dependent SOD in cortex and medulla was similar in rats on both dietary regimes.

These findings show that a short period of elevated dietary sodium intake increases NAD(P)H activity and protein levels in

the cortex and is associated with elevated 8-isoprostane excretion, consistent with a rise in ROS production. Importantly, the high salt intake did not change SOD activity and therefore scavenging potential. These observations support the view that this physiological challenge of high salt intake causes a modest oxidative stress.

Wilcox CS (2002). *Hypertension Reports* 4, 160-166

Where applicable, the authors confirm that the experiments described here conform with The Physiological Society ethical requirements.

PC11

High glucose affects structural and functional properties of human glomerular endothelial glycocalyx

A. Singh¹, V. Frieden², B. Haraldsson², P.W. Mathieson¹ and S.C. Satchell¹

¹*Academic Renal Unit, University of Bristol, Bristol, UK and*

²*Renal Unit, Sahlgrenska Academy, Gothenburg University, Gothenburg, Sweden*

Background:

The podocytes and the glomerular endothelial cells (GEnC) are the two cellular components of the glomerular filtration 'barrier'. We have recently shown that GEnC are covered by a thick layer of glycoproteins called glycocalyx which also acts as a selective sieve to the passage of protein suggesting its contribution to the 'barrier' to protein *in vivo*. Diabetes, recognized by high glucose levels, is the commonest condition leading to dysfunction of this barrier leading to leakage of protein in the urine.

Aims:

To test the effects of high glucose on the structural components of GEnC glycocalyx and examine its functional relevance by analysing its barrier properties to the passage of water and albumin.

Methods:

We used conditionally immortalised human GEnC developed in our laboratory. For all experiments comparisons were made between cells cultured in control medium (with 5.5mM glucose and 20mM mannitol) and high glucose medium (25mM glucose). Expression of proteoglycan core proteins syndecan 1 and 4, glypican-1, perlecan and versican was analysed by Western blotting. The expression of glycosaminoglycan chains was analysed by immunofluorescence and further quantified and characterized by radiolabelling studies (tritiated glucosamine and S³⁵). Barrier properties of GEnC monolayers were studied by real time trans-endothelial electrical resistance (TEER) and passage of labelled albumin.

Results:

High glucose reduced expression of total and sulphated glycosaminoglycan chains of glycocalyx by 55% and 62% respectively compared to controls ($n=4$, $p < 0.0001$). Immunofluorescence further confirmed reduction in the heparan sulphate chains with preservation of endothelial junctions. There was however no significant change in the expression of proteoglycan core proteins. Functional studies showed no changes in passage of water and solutes after high glucose but a significant increase in the

passage of labelled albumin by 30% relative to controls (n=10, p<0.001).

Conclusions:

High glucose milieu reduces the expression of sugar chains of glycocalyx without any alterations in their core proteins. This leads to a selective increase flux of albumin across GEnC monolayers without affecting the passage of water and solutes. These results support the role of GEnC glycocalyx in the pathophysiology of proteinuria in diabetes.

A.S. has received a training fellowship from Kidney Research UK.

Where applicable, the authors confirm that the experiments described here conform with The Physiological Society ethical requirements.

PC12

Cation channel activity of Band 3 (AE1) mutations in distal renal tubular acidosis

S.B. Walsh^{1,2}, H. Guizouarn², F. Borgese² and R.J. Unwin¹

¹Department of Physiology and Centre for Nephrology, University College London, London, UK and ²Bâtiment de Sciences Naturelles, Université de Nice-Sophia Antipolis, Nice, France

Hypokalemia is a common and incompletely explained finding in distal renal tubular acidosis (dRTA); its severity depending on the cause. Hereditary dRTA can be due to mutations in the anion exchanger 1 (AE1, Band 3). Recent work has shown that AE1 mutations associated with hereditary stomatocytosis (HSt) - an erythrocyte defect that can be a cause of pseudohyperkalemia - can behave as non-selective cation channels¹.

To investigate whether dRTA-causing AE1 mutants could also contribute to renal potassium wasting in dRTA via a similar mechanism, we studied 3 European autosomal dominant dRTA-causing mutants (R589H, G609R, S613F) and one Thai autosomal recessive mutant (G701D); each co-expressed with glycoporphin A (GPA - to enhance plasma membrane expression) in *Xenopus Laevis* oocytes.

Chloride influx experiments showed that anion transport activity is preserved and similar to wild type (wt), in contrast to the cation leaky HSt mutants described previously. However, rubidium (Rb⁺) influx experiments showed significantly higher cation flux in the western mutants compared with wt. Moreover, G701D had a very large cation flux, which was greatest at 0°C and was inhibited by stilbene AE1 inhibitors. These results were confirmed by measurement of intracellular cations: mutant-expressing oocytes, notably G701D, had reversal of intracellular cation concentrations compared with wt. In addition, when G701D was co-expressed with wt AE1 in the absence of GPA, a strong Rb⁺ flux was still found, indicating stability of the cation channel with heterodimer formation.

The G701D mutation is particularly frequent in NE Thailand², where dRTA and severe hypokalemia are endemic³, and hypokalemic paralysis, and sudden death, are unusually common^{4,5}. The novel behaviour of the AE1 mutants we have observed may contribute to potassium wasting in G701D homo and heterozygotes and thus add to the burden of hypokalemic disease seen in NE Thailand.

Bruce, L.J. *et al.* (2005) *Nature Genetics* **37**, 1258-1263.

Yenchitsomanus, P. T. *et al.* (2003) *Journal of human genetics* **48**, 451-456.

Nilwarangkur, S. *et al.* (1990) *The Quarterly journal of medicine* **74**, 289-301

Nimmannit, S. *et al.* (1991) *Lancet* **338**, 930-932.

Nademanee, K. *et al.* (1997) *Circulation* **96**, 2595-2600.

Where applicable, the authors confirm that the experiments described here conform with The Physiological Society ethical requirements.

PC13

P2 receptors in mouse cortical collecting duct revisited

E. Odgaard, H.A. Praetorius and J. Leipziger

Physiology and Biophysics, Aarhus University, Aarhus, Denmark

P2 receptors are functionally expressed along the distal renal tubule and their activation regulates Na⁺, K⁺ and H₂O transport^{1,2}. Strong evidence highlights a crucial role of the P2Y₂ receptor in this segment. Activation of luminal (and basolateral) P2Y₂ receptors inhibit ENaC-mediated Na⁺ absorption³ and global KO of this receptor causes augmented renal Na⁺ and H₂O absorption and increased systemic blood pressure⁴. In this study we used the isolated perfused tubule technique together with fluo-4 intracellular Ca²⁺ imaging in P2Y₂ WT and KO mice cortical collecting ducts to more comprehensively search for functionally relevant expression of luminal and basolateral P2 receptors. We find/confirm that luminal and basolateral ATP/UTP applied from either sides of the epithelium are potent agonists to trigger [Ca²⁺]_i increases. (WT % fluo-4 increase, luminal UTP: 56±9 and luminal ATP: 47±10; basolateral UTP: 32±7 and basolateral ATP: 26±4, n=5). In KO tubules the luminal and basolateral UTP effect were absent (KO % fluo-4 increase, luminal UTP: 3±1; basolateral UTP: 0±0, n=14). Intriguingly, despite the ineffectiveness of luminal UTP in P2Y₂ KO tubules, luminal ATP continued to trigger [Ca²⁺]_i increases, which amounted to about 50% of the WT luminal ATP response (KO % fluo-4 increase, luminal ATP: 19±5). Basolateral ATP-triggered [Ca²⁺]_i responses were reduced in KO tubules (KO % fluo-4 increase, ATP: 16±2). These results define that mouse cortical collecting ducts express luminal and basolateral P2Y₂ receptors. In addition, yet another luminal P2 receptor is present in this segment. Based on literature a P2X type receptor is suggested. The basolateral membrane is likewise equipped with at least one other P2 receptor, its nature remains to be established. These results extend the current state of knowledge of these receptors in the collecting duct and demand further in depth investigation of their functional relevance in salt and water handling.

1. Leipziger J (2003). *Am J Physiol Renal Physiol* **284**, F419-F432.

2. Unwin RJ, Bailey MA & Burnstock G (2003). *News Physiol Sci* **18**, 237-241.

3. Lehrmann H, Thomas J, Kim SJ, Jacobi C & Leipziger J (2002). *J Am Soc Nephrol* **13**, 10-18.

4. Rieg T, Bunday RA, Chen Y, Deschenes G, Junger WG, Insel PA & Valion V (2007). Mice lacking P2Y₂ receptors have salt-insensitive hypertension and facilitated renal Na⁺ and water excretion. *June, e-pub ahead.*

Where applicable, the authors confirm that the experiments described here conform with The Physiological Society ethical requirements.

PC14

Inhibition of the CFTR Cl⁻ channel by loop diuretics

M. Ju, T.S. Scott-Ward, Z. Cai and D.N. Sheppard

Department of Physiology and Pharmacology, University of Bristol, Bristol, UK

Loop diuretics are widely used to inhibit the Na⁺-K⁺-2Cl⁻ cotransporter (Haas & Forbush, 2000). However, Venglarik (1997) demonstrated that loop-diuretics inhibit the cystic fibrosis transmembrane conductance regulator (CFTR) Cl⁻ channel. To understand better how loop diuretics inhibit CFTR, we studied furosemide, bumetanide, and two other agents xipamide and piretanide, which are structurally related to furosemide and bumetanide, respectively. We recorded CFTR Cl⁻ currents in inside-out membrane patches excised from C127 cells expressing wild-type human CFTR. The pipette (external) solution contained 10 mM Cl⁻ and the bath (internal) solution contained 147 mM Cl⁻, 0.3 mM ATP and 75 nM PKA at 37°C; voltage was -50 mV. Data are means ± SEM of n observations and statistical analyses were performed using Student's paired t test.

When added to the internal solution, loop diuretics caused a reversible, concentration-dependent decrease in CFTR Cl⁻ current. For all agents tested, the concentration-response relationship was well fitted by the Hill equation with Hill coefficients of ~1. The rank order of potency for CFTR inhibition was xipamide ($K_i = 45 \pm 4 \mu\text{M}$) ≥ bumetanide ($K_i = 56 \pm 11 \mu\text{M}$) = piretanide ($K_i = 58 \pm 18 \mu\text{M}$) ≥ furosemide ($K_i = 71 \pm 15 \mu\text{M}$) (n = 5 for all agents).

To investigate further channel block, we used noise analysis. In the absence of furosemide, power density spectra of CFTR Cl⁻ currents were best fitted with two Lorentzian components with corner frequencies f_{c1} and f_{c2} of 1.17 ± 0.6 and 81 ± 10 Hz (n = 4), whereas in the presence of furosemide (100 μM), power density spectra were best fitted with three Lorentzian components with f_{c1} , f_{c2} and f_{c3} of 2.64 ± 1.38 , 63 ± 25 and 312 ± 107 Hz (n = 4), respectively, suggesting that f_{c3} corresponds to the rapid binding and dissociation of furosemide to and from individual CFTR Cl⁻ channels. Consistent with this idea, furosemide (100 μM) caused a flickery block of CFTR decreasing both open probability (P_o : control, 0.41 ± 0.03 ; furosemide (100 μM), 0.17 ± 0.02 ; n = 6; p < 0.01) and single-channel current amplitude (i: control, -0.76 ± 0.01 pA; furosemide (100 μM), -0.63 ± 0.03 pA; n = 6; p < 0.01). Thus, our data demonstrate that loop diuretics inhibit CFTR, their potency approaches that of the widely used CFTR blocker glibenclamide and that furosemide acts an open channel blocker of CFTR.

Haas M & Forbush III B (2000). *Ann Rev Physiol* **62**, 515-534.

Venglarik CJ (1997). *Pediatr Pulmonol Suppl* **14**, 230.

We thank Dishman Pharmaceuticals & Chemicals Ltd and Sanofi-Aventis for generous gifts of xipamide and piretanide, respectively. This work was supported by the CF Trust.

Where applicable, the authors confirm that the experiments described here conform with The Physiological Society ethical requirements.

PC15

Anion transport across planar lipid membranes by an artificial anionophore

G. Magro^{1,2}, L.W. Judd², D.N. Sheppard¹ and A.P. Davis²

¹Physiology, University of Bristol, Bristol, UK and ²Chemistry, University of Bristol, Bristol, UK

Natural and artificial ion transporters consisting of transmembrane channels or carriers are well known. Most of the synthetic transporters concern cation transport, whereas less interest has been shown in anion transport so far. In previous work (Koulov et al. 2003), we demonstrated that a family of small molecules derived from cholic acid termed 'cholapods' bind anions with high-affinity, promote Cl⁻ efflux from liposomes and ion transport across polarised MDCK epithelia (Koulov et al. 2003). Using excised inside-out membrane patches from giant liposomes, we compared the activity of cholapods with that of the cystic fibrosis transmembrane conductance regulator (CFTR) Cl⁻ channel under the same conditions. Addition of cholapods caused a concentration-dependent increase in Cl⁻ current, but no unitary events were observed.

We present here results obtained with a series of cholapods studied in planar lipid membranes (PLM). Membranes were formed by painting a mixture of POPE/Cholesterol (7/3) plus a known amount of cholapod. Using PLM, we have access to both sides of the membrane and thus to modify its environment. Thus, it has been possible to measure cholapod-mediated current under a series of conditions. Addition of cholapods in DMSO to the cis side of the membrane increased the observed current at an applied voltage (e.g. -100 mV). As the ion concentration was elevated the magnitude of cholapod-induced current saturated. Permeability experiments have been carried out and the transporters show good anion vs. cation selectivity, and also selectivity between anions. We interpret these data to suggest that cholapods can mediate anion transport across artificial lipid membranes by a carrier mechanism. Access to both sides of the membrane makes the PLM a potent technique to analyse the mechanism of action of synthetic anion transporters.

Koulov AV et al. (2003). *Angew Chem Int Ed Engl* **42**, 4931-4933.

Supported by the BBSRC, EU, CF Trust.

Where applicable, the authors confirm that the experiments described here conform with The Physiological Society ethical requirements.